Article ID: 1000-7032(2013)02-0165-06

Fano-like Resonances in Symmetric Planar Metamaterials

CAO Yang*

(*Department of Physics, Tongji University, Shanghai* 200092, *China*)

* *Corresponding Author, E-mail: caoyang*85@163.com

Abstract: The Fano-like resonance in symmetric planar metamaterials comprised of complimentary split ring resonators (CSRRs) is investigated by calculations from modal expansion method and transmission measurements. The Fano-like resonance is observed for one polarization with electric field component parallel to the mirror line of the structure, while only the broad dipole response can be found for the cross-polarization. Numerical simulations of field distributions reveal that the sharp response arises from the excitation of subradiant mode with nearly zero net dipole moment and poorly coupled with free space photons. The fast roll-off characteristic of Fano-like resonances is favorable for filtering and sensing applications.

Key words: Fano-like resonance; metamaterials; high quality factor

CLC number: O43 **Document code**: A **DOI**: 10.3788/fgxb20133402.0165

对称平面特异材料中的类 Fano 谐振

曹 扬*

(同济大学 物理系, 上海 200092)

摘要: 从理论和实验上研究了一种具有 C_3 对称性的平面特异材料中的类 Fano 谐振模式。该平面特异材料由互补劈裂开口环谐振器(CSRRs)周期排列而成,每个原胞包含 3 个缝隙,具有三度旋转对称性。当水平偏振的电磁波入射到该结构时,具有高品质因子的类 Fano 谐振模式可以被激励,透过率频谱上表现为尖锐的谐振峰。该类 Fano 谐振由单元内 3 个 CSRR 局域模式的平面内耦合形成的对称态和反对称态耦合产生,在传感器、滤波器方面有广阔的应用前景。

关 键 词: 类 Fano 谐振; 特异材料; 高品质因子

1 Introduction

Planar metamaterials, a class of thin slab structures periodically patterned with subwavelength metallic resonators, have provided a platform for observing various novel phenomena, ranging from extraordinary optical transmission[1], artificial magnetic atoms, to asymmetric transmission[2-5] and negative refraction[6-7]. Metamaterials are renowned for the ability to exhibit desired electromagnetic response in almost any frequency regime, which is not accessible for naturally materials. The planar design

收稿日期: 2012-12-24; **修订日期**: 2013-01-07
基金项目: 国家自然科学基金(10974144,11174221,11204218) 资助项目
作者简介: 曹扬(1985 -), 女, 安徽合肥人, 主要从事特异材料和表面等离激元光学的研究。
E-mail:caoyang85@163.com, Tel: (021)65989810

largely simplifies fabrication and composition of metamaterials, and simulates developments and applications in extensive fields.

Fano resonances were originally introduced in atomic physics, arise from the constructive and destructive interference of a discrete state with a continuum state. They are characterized by a distinct asymmetric lineshape with a pronounced minimum associated with a peak in the spectra[8]. Recently, the classical analogs of Fano resonances were reported in abundant plasmonic nanostructures and metamaterials[9-15], and have potential applications in filtering, sensing, and spasing[16].

The earliest Fano-like resonances in metamaterials are observed in a planar system with broken symmetry[17]. When excited by the electric field perpendicular to the mirror line of the asymmetric split ring resonators (SRRs), antiphase currents in two uneven arcs are established in a narrow frequency range, giving rise to a Fano-type characteristic in the reflection spectra. In plasmonic nanostructures, a family of closely arranged nanoparticles can exhibit Fano-like resonances without symmetry breaking[18-20]. The bonding/antibonding mode in the nanoparticle clusters provides the super-radiant/subradiant mode interacting to induce the highly dispersive response. As identical particles are used, the Fano-like resonances is derived only because of the symmetry of the structure. However, the nanostructures suffer from fabrication difficulties which require accurate control of the size, shape and arrangement of particles.

In this paper, we investigate the Fano-like resonances in complimentary split ring resonators (CSRRs) with C_3 rotational symmetry analogous to nanoparticle trimers. The CSRR is a negative structure of SRR, which replaces the metallic split rings with split ring slits etched in metal plate. The sharp resonant response is observed for the polarization with electric field component parallel to the mirror line of the structure, due to the nearly zero net dipole moment induced in the CSRR trimer. The proposed model system is fabricated by printed circuit boards and demonstrated in microwave regime. The findings are also valid in higher frequencies, and will have great potential in filtering and sensing applications.

2 Model and Analysis Method

Fig. 1 presents the schematic of our planar metamaterial. The metallic layer with a thickness of $t = 0.035$ mm is perforated with CSRR apertures in square lattice. The lattice constant is $p = 10$ mm. Each CSRR unit is made by etching three identical split ring slits through the metal film as illustrated in the enlarged schematic in Fig. 1. Inner and outer radii of CSRRs are $r = 3.8$ mm and $R = 4.8$ mm, respectively. The metallic strips separating the three split ring slits have a narrow width of $g = 0.2$ mm. The dielectric substrate has a thickness of $h = 1.575$ mm and a dielectric constant of $\varepsilon_r = 2.65$.

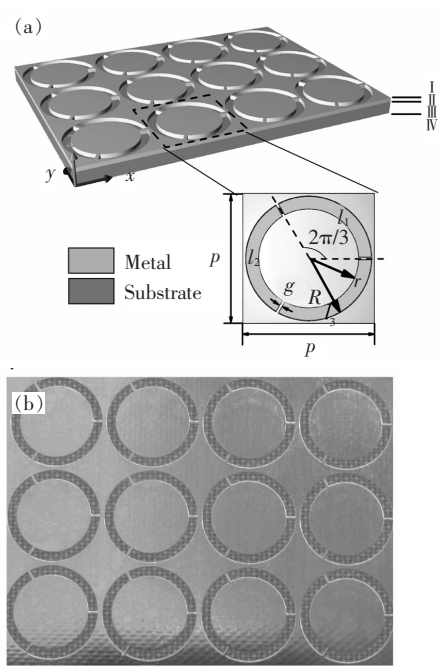

Fig. 1 (a) Schematic of the planar metamaterial consisting of CSRR aperture arrays and dielectric substrate. The dashed box indicates a unit cell formed by three split ring slits, which is enlarged to show detail. (b) The top view of the sample fabricated by a print current board.

With the assumption of perfect electric conductors (PECs) for metals in our model system, the transmission and reflection from the sample can be obtained by employing modal expansion method (MEM)[21-22]. The system can be divided into four

regions, from top to bottom, region Ⅰ ($z > h + t$) for the incident free space, region Ⅱ ($h < z < h + t$) containing the metallic layer, region Ⅲ ($0 < z < h$) consisting of dielectric substrate, region Ⅳ ($z < 0$) for the outgoing free space. It is worth noting that the electromagnetic fields in region Ⅱ cannot penetrate into the PEC walls in microwave regime, so that they only exist in the air holes and can be decomposed with a series of guided modes. We note that, owing to the in-plane mode orthogonality, only the $TE_{p,q}$ guided modes can be excited by the plane wave incidence, where the integer pair (p,q) in the subscript denotes a certain mode number, *i. e.* the $(p,q)^{\text{th}}$ order of the guided mode. As higher order guided modes decay rapidly, and have little contribution to transmission from the sample, only the lowest TE_{31} modes are considered in our calculation according to the structure symmetry. And the TE_{31} modes in each split ring slit are excited independently with no phase correlation with each other. As such we can write the electric field inside the apertures as the superposition of all the forward and backward TE_{31} modes:

$$\boldsymbol{E}^{\text{Ⅱ}} = \sum_{l=1}^{3} (a_l e^{-i\beta z} - b_l e^{i\beta z}) \boldsymbol{g}_l(x,y), \quad (1)$$

where $l = 1,2,3$ is the number of the three split ring slits in one unit cell. a_l and b_l are the coefficients of forward and backward guided waves, β is the wavevector component along z axis with $\beta = \sqrt{k_0^2 - T_{31}^2}$ and T_{31} being its corresponding in-plane wavevector component. k_0 is the wavevector in vacuum. T_{31} is the first root of eigen function in the waveguide. $\boldsymbol{g}_l(x,y)$ is the $(3,1)^{\text{th}}$ in-plane mode function of metallic apertures.

The electromagnetic fields in the incident side (region Ⅰ), the substrate (region Ⅲ) and the outgoing side (region Ⅳ) of the sample can be expanded with the superposition of Bloch waves:

$$\boldsymbol{E}^{\text{Ⅰ}} = \sum_{m=-\infty}^{+\infty} \sum_{n=-\infty}^{+\infty} \sum_{s=0,1} (I_s \delta_{m,n} e^{-ik_{z_{m,n}} z} + r_{m,n,s} e^{ik_{z_{m,n}} z}) \cdot \boldsymbol{P}_{m,n,s}(x,y) e^{-i(\boldsymbol{k}_{/\!/} + \boldsymbol{G}_{m,n}) \cdot \boldsymbol{r}_{/\!/}}, \quad (2)$$

$$\boldsymbol{E}^{\text{Ⅲ}} = \sum_{m=-\infty}^{+\infty} \sum_{n=-\infty}^{+\infty} \sum_{s=0,1} [(c_{m,n,s} e^{-ik'_{z_{m,n}} z} + d_{m,n,s} e^{ik'_{z_{m,n}} z}) \cdot \boldsymbol{Q}_{m,n,s}(x,y) e^{-i(\boldsymbol{k}_{/\!/} + \boldsymbol{G}_{m,n}) \cdot \boldsymbol{r}_{/\!/}}], \quad (3)$$

$$\boldsymbol{E}^{\text{Ⅳ}} = \sum_{m=-\infty}^{+\infty} \sum_{n=-\infty}^{+\infty} \sum_{s=0,1} t_{m,n,s} \boldsymbol{P}_{m,n,s}(x,y) \cdot e^{-i(\boldsymbol{k}_{/\!/} + \boldsymbol{G}_{m,n}) \cdot \boldsymbol{r}_{/\!/}} e^{-ik_{z_{m,n}} z}, \quad (4)$$

where $\boldsymbol{P}_{m,n,s}(x,y)$ and $\boldsymbol{Q}_{m,n,s}(x,y)$ are the unit vectors of electric fields at local point (x,y,z) for the x-polarized ($s = 0$) and y-polarized ($s = 1$) plane waves. $k_{z_{m,n}}$ and $k'_{z_{m,n}}$ are the z components of the wavevector in free space and dielectric substrate. I_s and $\boldsymbol{k}_{/\!/}$ are the coefficient and the in-plane wavevector of incident plane wave with $k_{z_{0,0}} = \sqrt{k_0^2 - |\boldsymbol{k}_{/\!/}|^2}$. $c_{m,n,s}$ and $d_{m,n,s}$ are the coefficients of forward and backward plane waves in the substrate. $r_{m,n,s}$ and $t_{m,n,s}$ are the coefficients of the $(m,n)^{\text{th}}$ reflected and transmitted Bloch waves. $\boldsymbol{G}_{m,n} = m\boldsymbol{b}_1 + n\boldsymbol{b}_2$ is the Bloch wavevector of square lattice. By applying the boundary continuum conditions, at the air/dielectric interface ($z = 0$), the metal/dielectric interface ($z = h$) and the metal/air interface ($z = h + t$), for the tangential components of electromagnetic fields, we derive the coefficients of the forward and backward guided waves within the structured layer, and those of the reflected and transmitted Bloch waves in free space.

3　Results and Discussion

We fabricate the sample by a printed circuit board as shown in Fig. 1(b). The lateral size of the sample is 300 mm × 300 mm. The transmission experiments are performed in microwave chamber with two pairs of directive horn antennas which are working at 8.2 ~ 12.4 GHz and 12.4 ~ 18.2 GHz respectively, fully covering the frequency range of interest. The two antennas are precisely aligned to measure the transmission under normal incidence. Our sample is placed in the middle between the horn emitter and the horn receiver.

In calculations and experiments, the plan wave incidence is propagating along negative z direction. Normal incidences with two orthogonal polarizations are theoretically calculated with MEM and measured in the microwave chamber, as shown in Fig. 2(a) and 2(c). We can see that the experimental measurements (circular dots) are in excellent agreement with theoretical predictions (solid lines). For y-

polarized ($\boldsymbol{E} /\!/ \hat{e}_y$) incidence, a broad dipole resonance at f = 13 GHz occurs in the spectrum (Fig. 2(a)). Under this polarization, the local resonances of the left split ring slit (l = 2) in the unit cells cannot be excited due to the mode orthogonality. We also calculate the transmission spectrum of the CSRR arrays with only the right two split ring slits (l = 1,3) in a unit cell as shown in Fig. 2(b). It is noted that the transmission spectrum with and without the left split ring slit (l = 2) are identical. For x-polarized ($\boldsymbol{E} /\!/ \hat{e}_x$) incidence, a Fano-like resonance at f = 10.5 GHz is observed beside a broad transmission peak centered at f = 12 GHz (Fig. 2(c)). For this polarization, all these three slits are excited by the x component of the incident wave. Transmission spectrum of the CSRR arrays with only the left slit or with only the right two slits are calculated and presented in Fig. 2(d). Further investigations will reveal that the Fano-like resonance is derived from the subradiant mode in CSRRs and can be explained by structure symmetry.

For better understanding of the physics of the

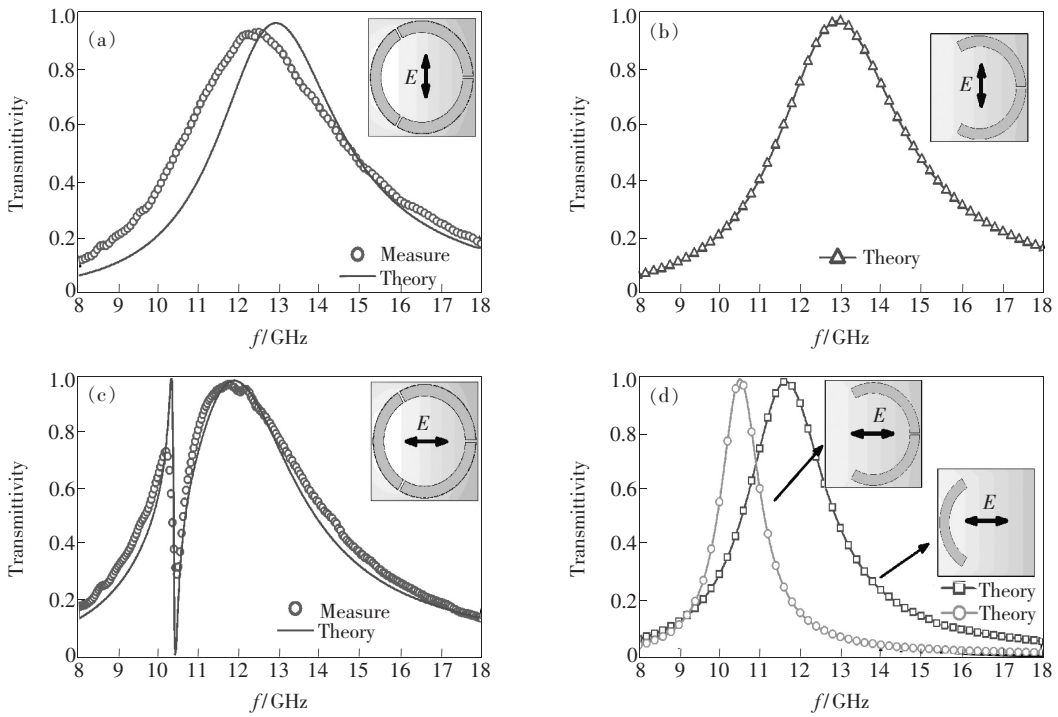

Fig. 2 Calculated (solid lines) and measured (circular dots) transmission under normal incidence with (a) and (b) y-polarized incidence, (c) and (d) x-polarized incidence. The sample and polarization are illustrated in insets accordingly.

Fano-like resonance, we calculate the field distributions on resonance by finite-difference-in-time-domain (FDTD) simulations as shown in Fig. 3. The electric field distributions in xy plane are presented by arrows, where the direction and length of an arrow denote the corresponding vector direction and amplitude of electric field at a local point. As the electric fields confined in the split ring slits are perpendicular to the slit edge and pointing to the center, each slit can be roughly regarded as an electric dipole. Under x-polarized incidence, all these three slits are excited with the x component of electric field. Owing to the structure symmetry, the dipole moment of the left split ring slit (l = 2) is almost equal in magnitude with that of the right two slits (l = 1,3), but oscillating in phase for the bonding mode (Fig. 3(a)) and out of phase for the antibonding mode (Fig. 3(b)). Thus the bonding mode exhibits a dipole response to the incident polarization and suffers from strong radiation loss. It shows up as a broad peak in the spectrum at f = 12 GHz. However, the antibonding mode possesses a nearly zero net dipole moment and behaves as a subradiant mode which induces a sharp Fano-like resonance at f = 10.5 GHz in the super-radiant continuum of the bonding mode. On the contrary, under y-polarized

incidence, the left slit can be hardly excited, as the electric field must be perpendicular to the long edge of the slit (Fig. 3(c)). Therefore the mode coupling and hybridization are absent, and only the broad dipole resonance is left in the spectrum at f = 13 GHz.

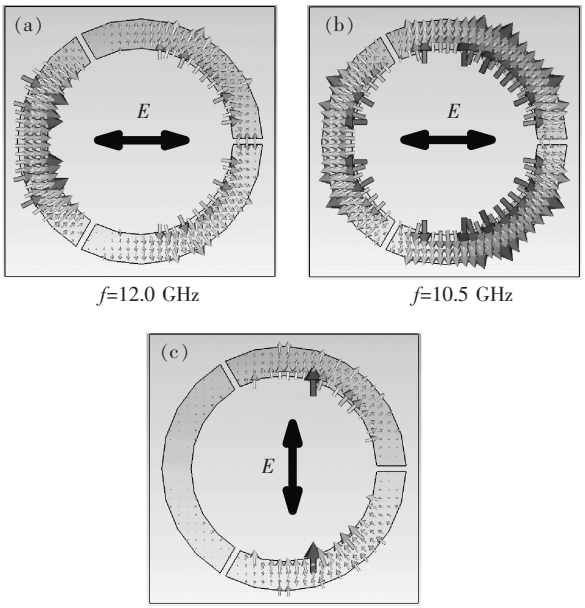

f=12.0 GHz　　f=10.5 GHz

f=13.0 GHz

Fig. 3　Calculated electric field distributions in xy plane for (a) x-polarized incidence at f = 12.0 GHz, (b) x-polarized incidence at f = 10.5 GHz, and (c) y-polarized incidence at f = 13.0 GHz.

4　Conclusion

In conclusion, we have theoretically and experimentally investigated the Fano-like resonance in planar metamaterials comprised of CSRRs which is an analog of nanoparticle trimers in plasmonics. The Fano-like response is observed for one polarization which is parallel to the mirror line of the trimer, while only the broad dipole response can be found for the cross-polarization. The underlying physics is revealed by the field distributions, which should be attributed to the structure symmetry and the nearly zero net dipole moment for the Fano-like resonance. The sharp response in spectrum is verified in microwave regime, but is also valid for THz, infrared and even in optical frequencies, and will have great potential in filtering and sensing applications.

References:

[1] Ebbesen T W, Lezec H J, Ghaemi H F, *et al.* Extraordinary optical transmission through sub-wavelength hole arrays [J]. *Nature*, 1998, 391(6668):667-669.

[2] Menzel C, Helgert C, Rockstuhl C, *et al.* Asymmetric transmission of linearly polarized light at optical metamaterials [J]. *Phys. Rev. Lett.*, 2010, 104(25):253902-1-4.

[3] Rogacheva A V, Fedotov V A, Schwanecke A S, *et al.* Giant gyrotropy due to electromagnetic-field coupling in a bilayered chiral structure [J]. *Phys. Rev. Lett.*, 2006, 97(17):177401-1-4.

[4] Zhao Y, Belkin M A, Alù A. Twisted optical metamaterials for planarized ultrathin broadband circular polarizers [J]. *Nat. Commun.*, 2012, 3(1):870.

[5] Wei Z Y, Cao Y, Fan Y C, *et al.* Broadband polarization transformation via enhanced asymmetric transmission through arrays of twisted complementary split-ring resonators [J]. *Appl. Phys. Lett.*, 2011, 99(22):221907-1-3.

[6] Pendry J B. Negative refraction makes a perfect lens [J]. *Phys. Rev. Lett.*, 2000, 85(18):3966-3969.

[7] Wei Z Y, Cao Y, Han J, *et al.* Broadband negative refraction in stacked fishnet metamaterial [J]. *Appl. Phys. Lett.*, 2010, 97 (14):141901-1-3.

[8] Miroshnichenko A E, Flach S, Kivshar Y S. Fano resonances in nanoscale structures [J]. *Rev. Mod. Phys.*, 2010, 82 (3):2257-2298.

[9] Lukʼyanchuk B, Zheludev N I, Maier S A, *et al.* The Fano resonance in plasmonic nanostructures and metamaterials [J]. *Nat. Mater.*, 2010, 9(9):707-715.

[10] Wu C H, Khanikaev A B, Adato R, *et al.* Fano-resonant asymmetric metamaterials for ultrasensitive spectroscopy and identification of molecular monolayers [J]. *Nat. Mater.*, 2012, 11(1):69-75.

[11] Al-Naib I A I, Jansen C, Koch M. Thin-film sensing with planar asymmetric metamaterial resonators [J]. *Appl. Phys. Lett.*, 2008, 93(8):083507-1-3.

[12] Al-Naib I A I, Jansen C, Koch M. High Q-factor metasurfaces based on miniaturized asymmetric single split resonators [J]. *Appl. Phys. Lett.*, 2009, 94(15):153505-1-3.

[13] Singh R, Al-Naib I A I, Koch M, *et al.* Asymmetric planar terahertz metamaterials [J]. *Opt. Exp.*, 2010, 18(12): 13044-13050.

[14] Jansen C, Al-Naib I A I, Born N, *et al.* Terahertz metasurfaces with high Q-factors [J]. *Appl. Phys. Lett.*, 2011, 98(5):051109-1-3.

[15] Singh R, Al-Naib I A I, Koch M, *et al.* Sharp Fano resonances in THz metamaterials [J]. *Opt. Exp.*, 2011, 19(7): 6312-6319.

[16] Zheludev N I, Prosvirnin S L, Papasimakis N, *et al.* Lasing spaser [J]. *Nat. Photon.*, 2008, 2(6):351-354.

[17] Fedotov V A, Rose M, Prosvirnin S L, *et al.* Sharp trapped-mode resonances in planar metamaterials with a broken structural symmetry [J]. *Phys. Rev. Lett.*, 2007, 99(14):147401-1-4.

[18] Fan J A, Bao K, Wu C H, *et al.* Fano-like interference in self-assembled plasmonic quadrumer clusters [J]. *Nano Lett.*, 2010, 10(11):4680-4685.

[19] Fan J A, Wu C H, Bao K, *et al.* Self-assembled plasmonic nanoparticle clusters [J]. *Science*, 2010, 328(5982):1135-1138.

[20] Sheikholeslami S N, Garcia-Etxarri A, Dionne J A. Controlling the interplay of electric and magnetic modes via fano-like plasmon resonances [J]. *Nano Lett.*, 2011, 11(9):3927-3934.

[21] Sheng P, Stepleman R S, Sanda P N. Exact eigenfunctions for square-wave gratings: Application to diffraction and surface-plasmon calculations [J]. *Phys. Rev.* B, 1982, 26(6):2907-2916.

[22] Lalanne P, Hugonin J P, Astilean S, *et al.* One-mode model and Airy-like formulae for one-dimensional metallic gratings [J]. *J. Opt.* A: *Pure Appl. Opt.*, 2000, 2(1):48-51.